Electronic Supplementary Material (ESI) for Journal of Materials Chemistry C.

Supporting Information

R. Wendt, B. Märker, A. Dubavik, A.-K. Herrmann, M. Wollgarten, Y. P. Rakovich, A. Eychmüller, K. Rademann and T. Hendel*

Versatile H_2O_2-driven mixed aerogel synthesis from CdTe and bimetallic noble metal nanoparticles

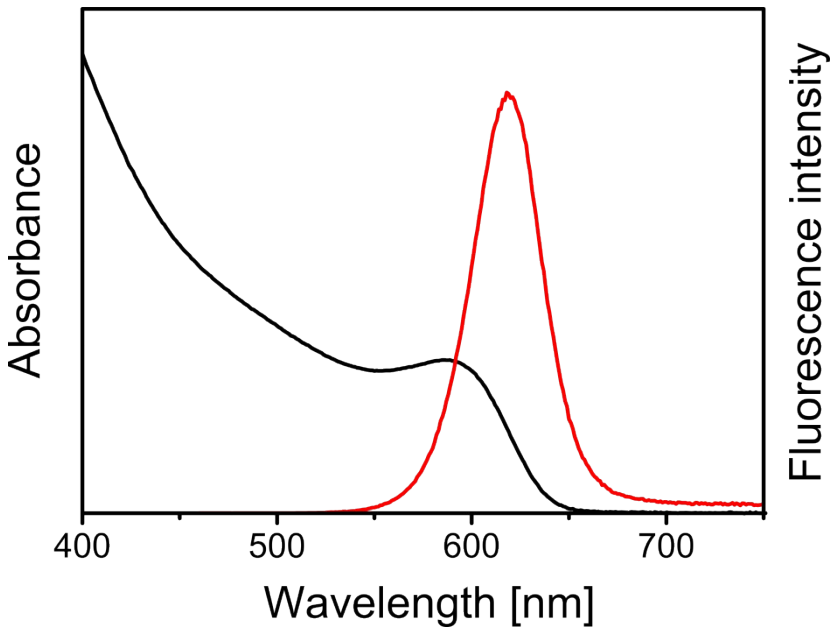

Fig. S1 UV-Vis absorption and fluorescence spectra of TGA-capped CdTe QDs.

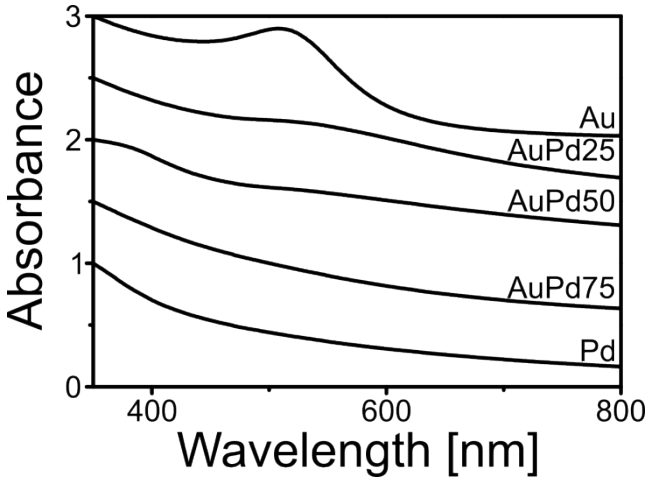

Fig. S2 Comparison of UV-Vis spectra of synthesized metal nanoparticles. Spectra are normalized and stacked for clarity.

Particle characterization and size determination from TEM analyses

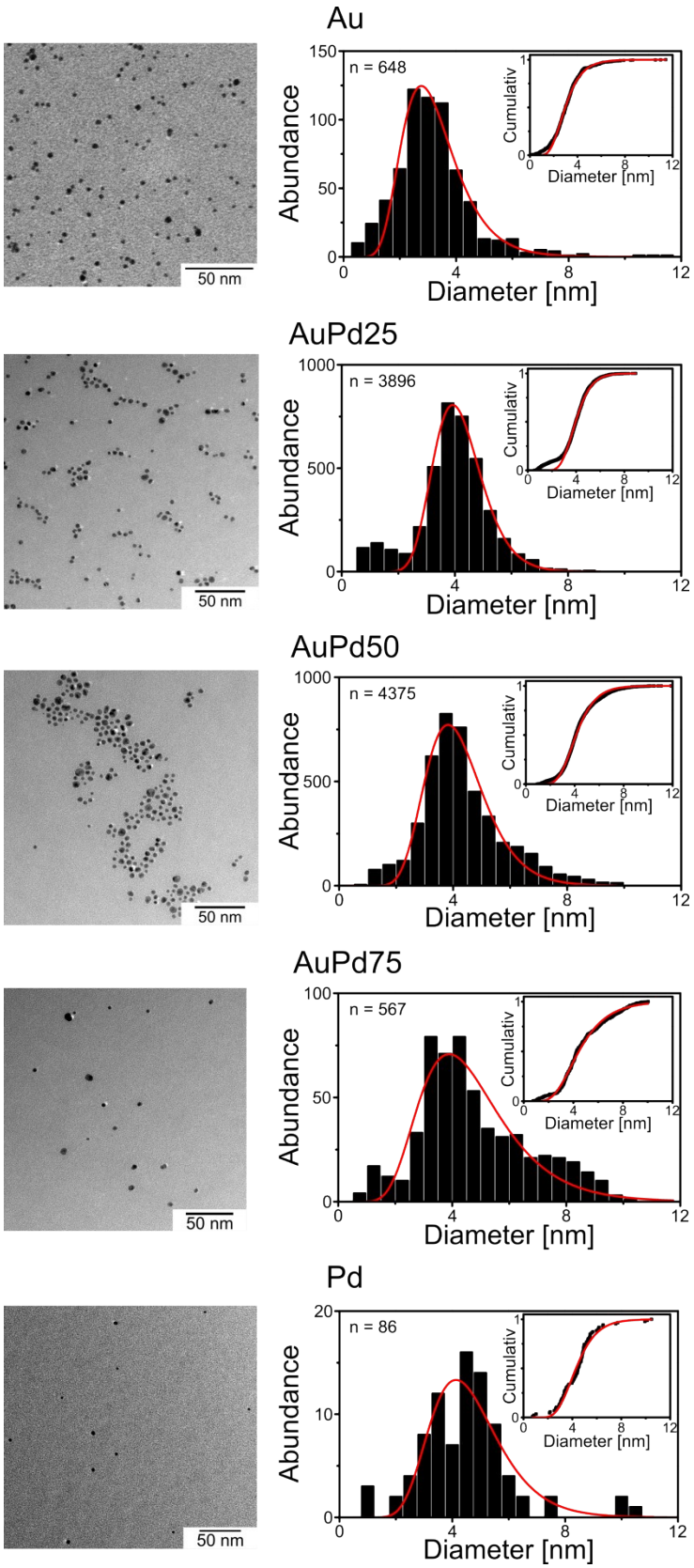

Fig. S3 TEM images (left) and numeric size evaluations (right) of prepared metal nanoparticle samples. The histograms are fitted with a log-normal function. Insets: Cumulative plots are used to derive the mean particle diameters.

For automated quantification we used the following procedure. A detailed description will be the object of our future publications:

Normalization: Image intensities were normalized to the interval [0.0, 1.0].

Background subtraction: Background subtraction was done by fitting a two dimensional second order polynomial to a subset of image pixels comprised of every 16th pixel in both image dimensions. This first estimate of the background function was subtracted from the original image. Then, the fit procedure was repeated for this corrected image and the resulting polynomial was added to the background function. This process was repeated until the total amplitude of the polynomial correcting the background function became smaller than 10^{-6}.

Image modeling and segmentation: In the next step, a set of averaged images was calculated from the background corrected image using circular kernels of increasing diameter. Each pixel inside the kernel contributed equally to the respective average value. For each averaged image $\{x_{i,2}\}$ we calculated the two dimensional intensity histogram using the non-averaged background corrected image $\{x_{i,1}\}$ for the second histogram dimension. Then a set of two-dimensional Gaussians was used to model the histograms:

$$p_k(\mathbf{x}_i|\boldsymbol{\mu}_k, \Sigma_k) = \frac{1}{2\pi\sqrt{\det(\boldsymbol{\Sigma}_k)}} \exp\left[-\frac{1}{2}\left(\mathbf{x}_i - \boldsymbol{\mu}_k\right)^T \Sigma_k^{-1}\left(\mathbf{x}_i - \boldsymbol{\mu}_k\right)\right] \quad (1)$$

Herein, $p_k(x_i \,|\, \mu_k, \Sigma_k)$ is the probability density for that pixel with index i, the intensity pair $[x_{i,1}, x_{i,2}] = x_i$ given the mean values $[\mu_{k,1}, \mu_{k,2}] = \mu_k$ and covariance matrix Σ_k. Index k numbers the individual Gaussians of the set. Here, we used three Gaussians ($K = 3$), whereas the smallest $\mu_{k,1}$ shall represent the intensity value of the particles (i.e., dark particles on bright background). In principle, expectation maximization could be employed to infer the parameters of the Gaussians. However, this will not allow to deduce an error metric, which is needed for our algorithm (see below). Thus, we extended our model by an indicator function $z_k(x_i)$ which adopts the value 1 if pixel i belongs to Gaussian of index k, otherwise it is zero. This leads to

$$p_k(\mathbf{x}_i|\boldsymbol{\mu}_k, \Sigma_k, z_k) = \prod_{k=0}^{K-1}\left(\frac{1}{2\pi\sqrt{\det(\boldsymbol{\Sigma}_k)}} \exp\left[-\frac{1}{2}\left(\mathbf{x}_i - \boldsymbol{\mu}_k\right)^T \Sigma_k^{-1}\left(\mathbf{x}_i - \boldsymbol{\mu}_k\right)\right]\right)^{z_k} \quad (2)$$

Eventually, the parameters were inferred by the following iterative procedure. The indicator function z_k was preset with random values. Then, the parameters of the Gaussians were calculated using

$$\mu_{k,j}^{(n+1)} = \frac{\sum_i z_k^{(n)}(x_i) x_{i,j}}{\sum_i z_k^{(n)}(x_i)} \quad (3)$$

for the centers and the components (j, h) of the covariance matrix according to

$$\Sigma_k^{(n+1)} = \frac{\sum_i z_k^{(n)}(x_i)(x_{i,j} - \mu_{k,j}^{(n+1)})(x_{i,h} - \mu_{k,h}^{(n+1)})}{\sum_i z_k^{(n)}(x_i)} \tag{4}$$

We completed the iteration by assigning new values to $z_k^{(n+1)}(x_i)$ with probabilities $p_k(x_i \mid \mu_k, \Sigma_k)$ and started over with equation 4.

Initially, iterations were repeated until the Gaussian parameters adopted stable values (so-called burn-in phase). Then iterations were continued for a given number of times and each version of the indicator function was stored. Image segmentation was provided by choosing the assignment according to

$$c_i = \underset{k}{\operatorname{argmax}} \left(\sum_{n=0}^{N-1} z_k^{(n)}(x_i) \right) \tag{5}$$

where the sum extends over all iterations.

Segmentation assessment: To assess the fidelity of the segmentation, the segmentation entropy[1] was calculated for each pixel according to

$$S(x_i) = \frac{1}{\log(K)} \sum_{k=0}^{K-1} q_k(x_i) \log(q_k(x_i)) \tag{6}$$

with $K = 3$ and

$$q_k(x_i) = \left(\frac{\sum_{n=0}^{N-1} z_k^{(n)}(x_i)}{N} \right) \tag{7}$$

The prefactor $1/\log(K)$ normalizes $S(x_i)$ to the interval [0, 1], whereas the value of 1 is obtained if all probabilities are equal, i.e. $q_k = 1/K$. Highest fidelity is reached for $S(x_i) = 0$. In this case a single probability has value 1 and all other values are zero. The case of three probability distributions, $q_1(x_i) > q_2(x_i) \geq q_3(x_i)$ (and permutations in k) is unambiguous. However cases such as i.e. $q_1(x_i) = q_2(x_i) > q_3(x_i)$ (and permutations in k) are ill-posed. As one probability depends on the other two, the entropy can be represented in a triangular color coded map. This is visualized in Figure S4a. The red (inner) area marks probability combinations that have to be rejected. Indeed, some tolerance is introduced by regarding probabilities as equal if the values differ less than 0.3. The green (outer) areas indicate valid combinations.

The lowest entropy value for this scenario is obtained for $p_0 = p_1 = \frac{1}{2} > p_2 = 0$. Here, $S(x_i)$ adopts the value of $S(x_i) = S_{limit} = \frac{\log(2)}{\log(3)} \cong 0.63$. Here, we adopted a more conservative rule that rejects all cases where the entropy is larger than 0.5 S_{limit}. This area is shown in Fig. S4b.

Choice of averaging kernel: We calculated the mean entropy per pixel, $\hat{S}$, for the ensemble of particle pixels and plotted it as a function of increasing kernel size. In general, the curve initially

drops to a minimum value and then rises again. We chose the kernel that yields the minimum value of $\hat{S}$. We found that an initial increase of the curve is observed, if the burn-in phase is too short and/or the step size between two subsequent kernel sizes is too large.

Quantification of particle sizes: A binarized particle image was then achieved by selecting all pixels of the intensity class (equation 6) which had lowest $\mu_{k,1}$ and fulfilled the entropy criterion. In this binary image, particles were identified and their area was determined. Their radius was calculated assuming circular shaped particles.

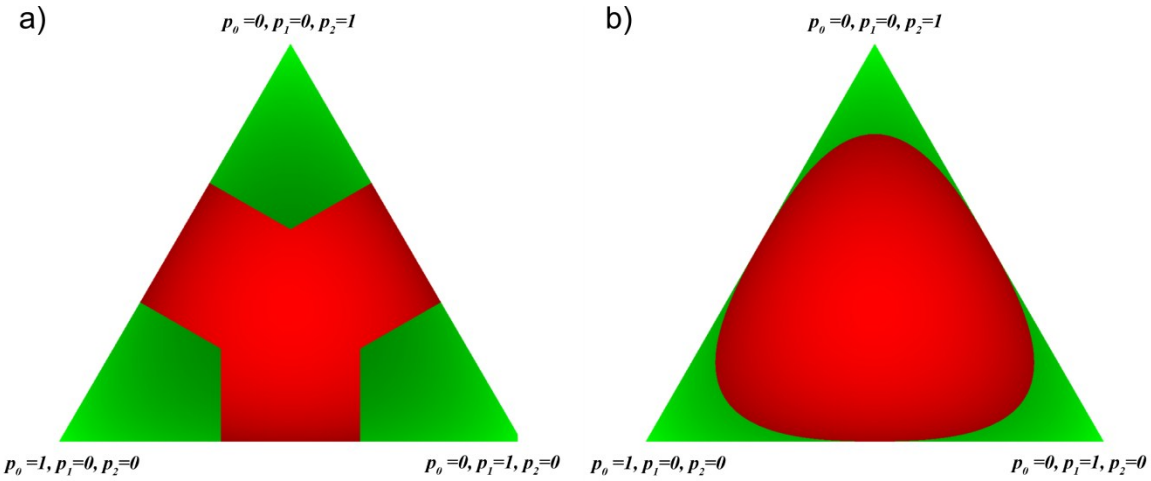

Fig. S4 Visualization of the segmentation entropy. (a) Invalid area: $|p_{mod\,(i,3)} - p_{mod\,(i+1,3)}| < 0.3 \wedge (p_{mod\,(i,3)} \vee p_{mod\,(i+1,3)}) > 0.85 p_{mod\,(i+2,3)}$. (b) Invalid area for $S(x_i) = \frac{\log(2)}{\log(3)} \cong 0.63$.

Mean particle diameters were determined using the cumulative distribution function of the log-normal distribution (equation (8)) as a fit function.

$$f(x) = \frac{1}{2}\left[1 + erf\left(\frac{lnx - \mu}{\sigma\sqrt{2}}\right)\right] \quad (8)$$

Table S1: Synthesized metal nanoparticle samples and their mean particle diameter (d) determined from TEM analysis using fit parameters σ and μ from the cumulative distribution function (equation 8).

sample	d [nm]	σ	μ
Au	3.2	0.364	1.089
AuPd25	4.1	0.254	1.375
AuPd50	4.3	0.298	1.416
AuPd75	4.8	0.401	1.492
Pd	4.5	0.309	1.457

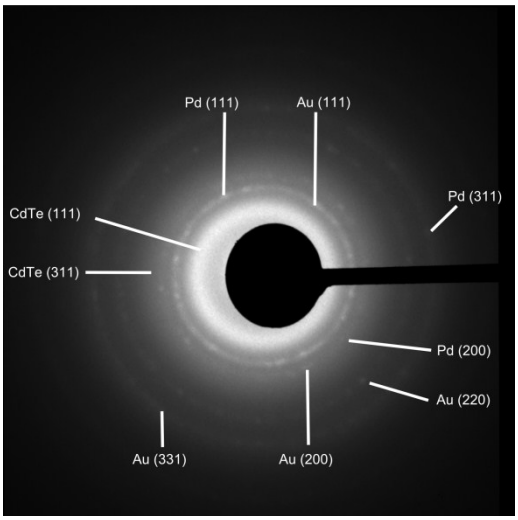

Fig. S5 Selected area electron diffraction pattern of aerogel sample CdTe/AuPd25 40:1 (H_2O_2).

Table S2: Summary of the evaluated data of synthesized gels from H_2O_2 and photochemical destabilization (PD) for different metal nanoparticles and a variation of the CdTe to metal particle ratio. The duration of the treatment representing a successful gelation is given. (-) symbolizes a system that was not tested. (*) can be found in the work of T. Hendel et al. Adv. Funct. Mater. 2013, ***23****, 1903*

mixed	160:1		80:1		40:1		14:1	
gels	H_2O_2	PD	H_2O_2	PD	H_2O_2	PD	H_2O_2	PD
CdTe/Au	36 h	*	26 h	*	18 h	*	24 h	*
CdTe/AuPd25	24 h	80 min	21 h	115 min	26 h	60 min	36 h	120 min
CdTe/AuPd50	-	85 min	-	85 min	-	90 min	-	100 min
CdTe/AuPd75	-	80 min	-	80 min	-	70 min	-	60 min
CdTe/Pd	22 h	70 min	24 h	60 min	28 h	55 min	168 h	no gel

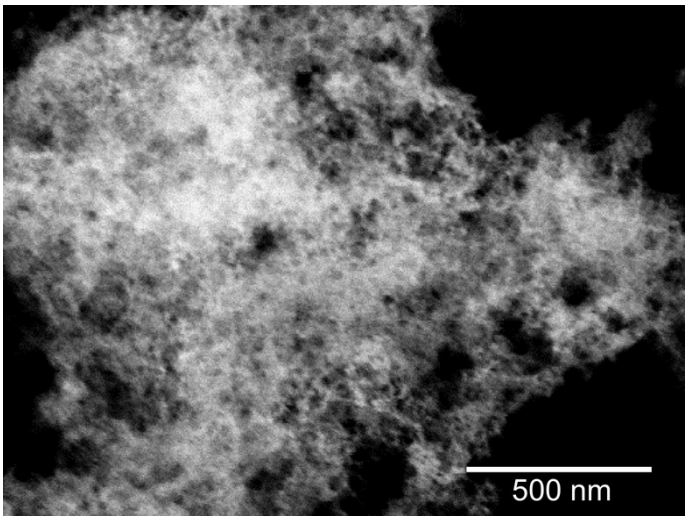

Fig. S6 Representative STEM image of the aerogel sample CdTe/AuPd25 40:1 (H_2O_2) used for EDX-based elemental analysis.

Table S3: Results of the elemental analysis of the aerogel sample CdTe/AuPd25 40:1 (H_2O_2) from three STEM-EDX measurements at lower resolution.

Element series	Net counts	Net count error	Atom-%	Atom-% error
Measurement #1				
Cd-L	6485	± 90	**52.5**	± 0.7
Te-L	3816	± 70	**28.5**	± 0.5
S-K	794	± 34	**13.0**	± 0.6
Au-M	612	± 33	**2.6**	± 0.1
Pd-L	391	± 40	**3.4**	± 0.3
Measurement #2				
Cd-L	6942	± 94	**53.4**	± 0.7
Te-L	3947	± 74	**28.0**	± 0.5
S-K	920	± 37	**14.3**	± 0.6
Au-M	509	± 33	**2.1**	± 0.1
Pd-L	272	± 38	**2.2**	± 0.3
Measurement #3				
Cd-L	11888	± 122	**52.5**	± 0.5
Te-L	7160	± 96	**29.2**	± 0.4
S-K	1432	± 44	**12.7**	± 0.4
Au-M	946	± 40	**2.2**	± 0.1
Pd-L	729	± 50	**3.4**	± 0.2

The mean Cd:Au ratio from the three STEM-EDX measurements was calculated as 23.1:1. Accordingly, the mean Pd:Au ratio in the aerogel is 1.3:1.

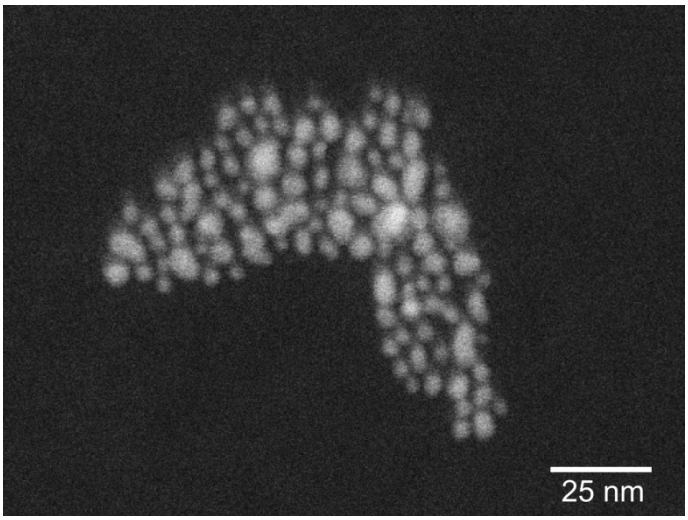

Fig. S7 Representative STEM image of bimetallic AuPd25 used for EDX-based elemental analysis.

Table S4: Results of elemental analysis of bimetallic AuPd25 nanoparticles from STEM-EDX measurements.

Element series	Net counts	Net count error	Atom-%	Atom-% error
Measurement #1				
Au-M	993	± 43	**43.1**	± 1.8
Pd-L	604	± 41	**56.9**	± 3.5
Measurement #2				
Au-M	921	± 37	**45.2**	± 1.8
Pd-L	557	± 32	**54.8**	± 3.2
Measurement #3				
Au-M	228	± 19	**44.9**	± 3.7
Pd-L	142	± 18	**55.1**	± 6.9
Measurement #4				
Au-M	603	± 34	**40.1**	± 2.1
Pd-L	440	± 31	**59.9**	± 3.9
Measurement #5				
Au-M	403	± 24	**49.7**	± 3.0
Pd-L	209	± 20	**50.3**	± 4.8
Measurement #6				
Au-M	993	± 43	**45.8**	± 5.9
Pd-L	604	± 41	**54.2**	± 11.0

The mean Pd:Au ratio in the initial bimetallic AuPd25 nanoparticles is 1.2:1.

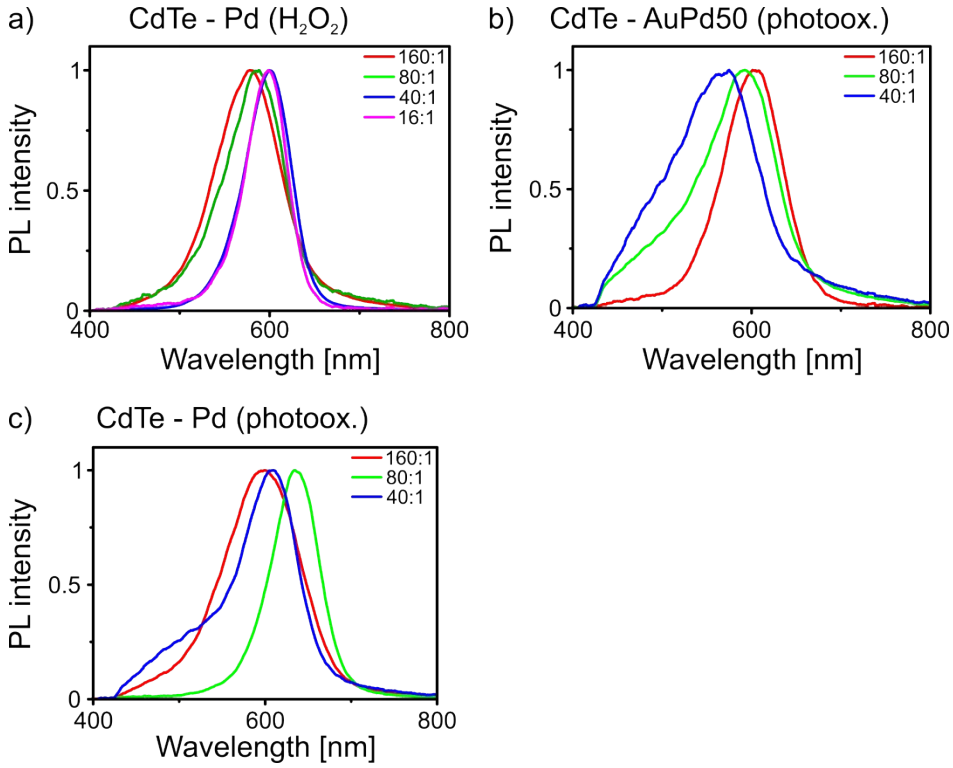

Fig. S8 PL spectra of mixed aerogels with varying composition obtained from the two different gelation methods: (a) CdTe/Pd aerogels obtained by H_2O_2 destabilization, (b) CdTe/AuPd50 aerogels obtained by photooxidation method and (c) CdTe/Pd aerogels obtained from photooxidation method.

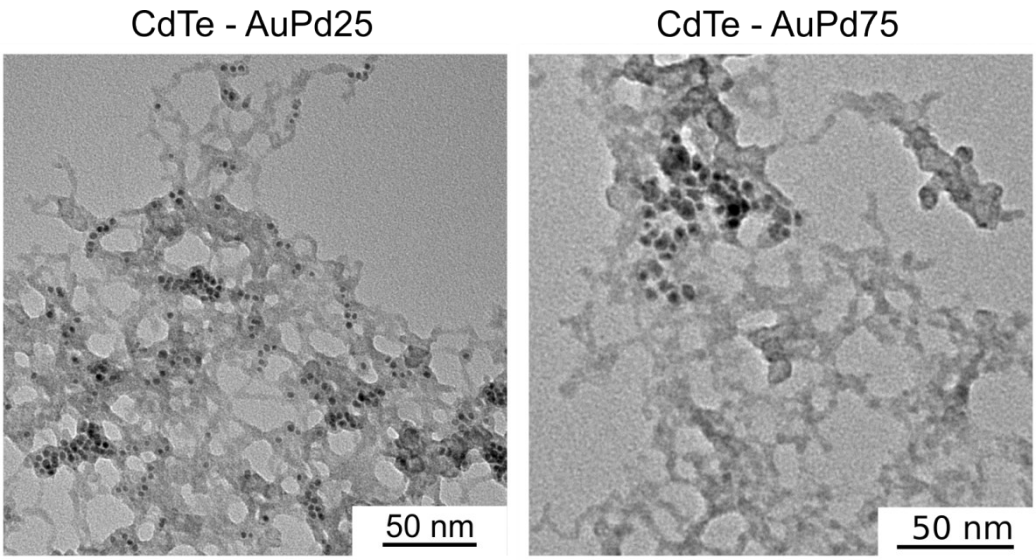

Fig. S9 TEM images of mixed aerogels obtained from photooxidation method containing CdTe and different metallic nanoparticles.

REFERENCES

(1) Wollgarten, M.; Habeck, M. Autonomous Reconstruction and Segmentation of Tomographic Data. *Micron* **2014**, *63*, 20–27.